VNN1 overexpression in pancreatic cancer cells inhibits paraneoplastic islet function by increasing oxidative stress and inducing β-cell dedifferentiation

WENJIE QIN[1], MUXING KANG[2], CHAO LI[2], WEN ZHENG[2] and QINGQU GUO[2]

[1]Department of Hepatobiliary and Pancreatic Surgery, The First Affiliated Hospital of Zhengzhou University, Zhengzhou, Henan 450052; [2]Department of Surgery, The Second Affiliated Hospital, Zhejiang University School of Medicine, Hangzhou, Zhejiang 310009, P.R. China

Received December 31, 2022; Accepted April 3, 2023

DOI: 10.3892/or.2023.8557

Abstract. Vanin-1 (VNN1) may be a potential biomarker for the early screening of pancreatic cancer (PC)-associated diabetes (PCAD). A previous study by the authors reported that cysteamine secreted by VNN1-overexpressing PC cells induced the dysfunction of paraneoplastic insulinoma cell lines by increasing oxidative stress. In the present study, it was observed that both cysteamine and exosomes (Exos) secreted by VNN1-overexpressing PC cells aggravated the dysfunction of mouse primary islets. PC-derived VNN1 could be transported into islets through PC cell-derived Exos (PC-Exos). However, β-cell dedifferentiation, and not cysteamine-mediated oxidative stress, was responsible for the islet dysfunction induced by VNN1-containing Exos. VNN1 inhibited the phosphorylation of AMPK and GAPDH, and prevented Sirt1 activation and FoxO1 deacetylation in islets, which may be responsible for the induction of β-cell dedifferentiation induced by VNN1-overexpressing PC-Exos. Furthermore, it was demonstrated that VNN1-overexpressing PC cells further impaired the functions of paraneoplastic islets *in vivo* using diabetic mice with islets transplanted under the kidney capsule. On the whole, the present study demonstrates that PC cells overexpressing VNN1 exacerbate the dysfunction of paraneoplastic islets by inducing oxidative stress and β-cell dedifferentiation.

Correspondence to: Dr Wenjie Qin, Department of Hepatobiliary and Pancreatic Surgery, The First Affiliated Hospital of Zhengzhou University, 1 Jianshe Road, Zhengzhou, Henan 450052, P.R. China
E-mail: qinwenjie0214@zzu.edu.cn

Abbreviations: VNN1, Vanin-1; PCAD, pancreatic cancer-associated diabetes; Exos, exosomes; ROS, reactive oxygen species; PPARγ, peroxisome proliferator-activated receptor γ; GSH, glutathione; AMPK, AMP-activated protein kinase; GAPDH, glyceraldehyde 3-phosphate dehydrogenase; Sirt1, sirtuin 1; FoxO1, Forkhead box protein O1

Key words: VNN1, pancreatic cancer-associated diabetes, oxidative stress, exosomes, β-cell dedifferentiation

Introduction

Pancreatic cancer (PC), usually occurring as pancreatic ductal adenocarcinoma, is a common malignant digestive tumor, which is characterized by silent onset, rapid progress and a poor prognosis (1,2). The onset of secondary diabetes caused by PC, which is termed as PC-associated diabetes (PCAD), occurs almost 10-13 months prior to the diagnosis of PC (3-5), indicating that PCAD may be used as an early clinical manifestation for PC screening. Therefore, it is noteworthy to explore the pathogenesis and search for specific biomarkers of PCAD.

Vanin-1 (VNN1) is anchored to the cellular membrane with pantetheinase activity, which hydrolyzes pantetheine to produce cysteamine (6-8). VNN1 can promote oxidative stress and the inflammatory response (9). Additionally, VNN1 has been confirmed to be overexpressed in cancer tissues of patients with PCAD and can be used as a blood biomarker for the discrimination of PCAD from type 2 diabetes (10). A previous study by the authors also demonstrated that VNN1 was overexpressed in neoplastic cells in the majority of cases of PCAD (11). Furthermore, the authors previously co-cultured VNN1-overexpressing human PC cell lines with insulinoma cell lines (INS-1 and β-TC-6), and examined the effects of the overexpression of VNN1 on insulinoma cells and explored the underlying mechanisms (11). It was demonstrated that the extracellular cysteamine concentration of VNN1-overexpressing PC cells was markedly increased, which aggravated oxidative stress in paraneoplastic insulinoma cells by upregulating reactive oxygen species (ROS) levels and downregulating the peroxisome proliferator-activated receptor γ (PPARγ)/glutathione (GSH) concentrations, and ultimately, the viability and function of insulinoma cells were impaired more significantly (11). Therefore, VNN1 may participate in the pathogenesis of PCAD and may be used as a specific biomarker of PCAD for the early diagnosis of PC.

Exosomes (Exos) are encapsulated by a bilayer lipid membrane and contain a variety of bioactive molecules, such as DNA, RNA, protein, and can be used as the intercellular

conveyance medium of molecules and signal pathways (12). PC cells secrete a large amount of Exos into the surrounding microenvironment, which causes paraneoplastic β-cell dysfunction (13). Moreover, PC cell-derived Exos (PC-Exos) can impair the functions of skeletal muscle cells, adipocytes and intestinal mucosal cells, leading to decreased insulin secretion and insulin resistance (14-17).

In the present study, mouse primary islets were used for more accurately researching the effects of VNN1-overexpressing PC cells on paraneoplastic β-cells. The results revealed that VNN1-overexpressing PC cells could also inhibit the viability and function of islets by increasing oxidative stress. In addition, for the first time, to the best of our knowledge, it was found that VNN1-overexpressing PC-Exos could induce β-cell dedifferentiation, which further reduced the insulin secretion of islets. Thus, the present study also aimed to explore the potential underlying mechanisms. Furthermore, islets were transplanted under the kidney capsule of diabetic mice in order to observe the effects of islets co-cultured with VNN1-overexpressing PC cells on blood glucose regulation *in vivo*.

Materials and methods

Cell culture and islet isolation. The human PC cell lines, PANC-1 (cat. no. TCHu98) and CFPAC-1 (cat. no. TCHu112), were purchased from The Cell Bank of Type Culture Collection of the Chinese Academy of Sciences and cultured in RPMI-1640 medium (cat. no. 11875119; Gibco; Thermo Fisher Scientific, Inc.) supplemented with 10% fetal bovine serum (FBS; cat. no. 12484028; Gibco; Thermo Fisher Scientific, Inc.) and 100 IU/ml penicillin and streptomycin (cat. no. 450-201-EL; Wisent, Inc.), at 37˚C in a humid atmosphere (5% CO_2 and 95% air). Pancreatic islets were isolated from C57BL/6J (B6) mice as previously described (18). All animal experiments in the present study were approved by the Animal Ethics Committee of The First Affiliated Hospital of Zhengzhou University, Zhengzhou, China (Ethics no. 2018-03-003) and conducted in accordance with the approved guidelines. A total of 150 B6 mice (female; 4-6 weeks old; weighing 18-20 g; Jackson Laboratory) were used for islet isolation. These B6 mice were housed in a specific pathogen-free (SPF) environment under a 12-h light/dark cycle with *ad libitum* access to food and water at 24˚C and 55% humidity. The B6 mice were sacrificed by cervical dislocation following anesthesia by isoflurane inhalation (2-6% for induction; 1-3% for maintenance), and 2.5 ml collagenase (type V, 2.0 mg/ml; cat. no. 40511ES60; Yeasen Biotechnology Co., Ltd.) was injected into the common bile ducts of these mice, and the distended pancreas was then harvested and incubated in a shaking water bath at 37˚C for 15 min. Purified islets were obtained by Ficoll (Ficoll PM400; cat. no. F4375; Sigma-Aldrich Trading Co., Ltd.) gradient centrifugation at 3,000 x g for 20 min at 4˚C and cultured in HAM's F10 medium (cat. no. 11550043; Gibco; Thermo Fisher Scientific, Inc.). One islet equivalent (IEQ) was calculated as previously described (19).

Lentiviral vector transfection. A full-length human VNN1 cDNA was cloned into a lentiviral vector (Shanghai GeneChem Co., Ltd.) for constitutive gene expression. The lentiviral vector was co-transfected with packaging vectors (Shanghai GeneChem Co., Ltd.) into 293T cells (cat. no. GNHu17; from The Cell Bank of Type Culture Collection of the Chinese Academy of Sciences). The PANC-1 and CFPAC-1 cells were infected with empty or VNN1-expressing lentiviruses. The PANC-1 and CFPAC-1 cells with a stable overexpression of VNN1 were termed as PV and CV, and the PANC-1 and CFPAC-1 cells transfected with the empty vector were referred to as PE and CE.

Establishment of co-culture system. The lower and upper compartments of Transwell chambers (6-well; cat. no. 3412; Corning, Inc.) were separated by polyvinylpyrrolidone-free polycarbonate filters (pore size, 0.4 μm). Each lower compartment was seeded with islets (200 islets/well), and the upper compartment was loaded with PC cells ($2x10^5$ cells/well).

Cell viability assay. PC cell viability was determined using MTT assay (cat. no. CT01-5; MilliporeSigma). Cells seeded in a 96-well plate were treated with MTT for 4 h, and after removing the supernatant, DMSO (cat. no. 94563; MilliporeSigma) was added to each well. After shaking the plate, an ELISA reader (BioTek Instruments, Inc.) was used to measure the optical density value at 570 nm. Islets were pre-treated with 10 μM GSH (cat. no. G4251; MilliporeSigma) or 10 μM thiazolidinedione (TZD; cat. no. 375004; MilliporeSigma) for 2 h at 37˚C. Islets not pre-treated with GSH or TZD were used as controls. Following gentle agitation for 5 min in calcium-free medium containing Trypsin/EDTA (cat. no. T4049; MilliporeSigma) at in a water bath at 37˚C, islets were dissociated into single cells, and single cells were then cultured in HAM's F10 medium (cat. no. 11550043; Gibco; Thermo Fisher Scientific, Inc.); single cells were stained with 0.4% Trypan blue (cat. no. T6146; MilliporeSigma) for 3 min at room temperature and cell viability was determined by counting the live and dead cells using a hemocytometer (cat. no. MDH-2N1; MilliporeSigma) under a light microscope (Olympus IX-71; Olympus Corporation).

Isolation and characterization of Exos. After the PC cells grew to 80% confluency, the supernatants were replaced by medium with exosome-free FBS (differential centrifugation at 100,000 x g for 16 h at 4˚C). Supernatants were collected following culture for 48 h, and Exos were then isolated from the supernatants using differential centrifugation as previously described (14). A transmission electron microscope (Philips Healthcares) and Zetasizer Nano ZS (Malvern Instruments, Ltd.) were used to characterize the Exos. Exos isolated from the PANC-1, PE and PV cells were termed as PANC1-Exos, PE-Exos and PV-Exos, respectively.

Western blot analysis. Western blot analysis procedures were performed in accordance with standard protocols (14). Total protein was extracted from PC cells, islets and Exos using RIPA lysis buffer (cat. no. R0278; MilliporeSigma) supplemented with a protease inhibitor cocktail (cat. no. P8340; MilliporeSigma). Nuclear and cytoplasmic proteins were extracted using NE-PER Nuclear and Cytoplasmic Extraction Reagents (cat. no. 78833; Thermo Fisher Scientific, Inc.) Protein concentrations were quantified using the BCA Protein Quantification kit (cat. no. 23225; Thermo Fisher Scientific, Inc.).

The protein lysates (30 μg/lane) were separated by 10% SDS-polyacrylamide gels and transferred to polyvinylidene difluoride membranes (cat. no. ISEQ00010; MilliporeSigma). The membranes were blocked with 5% skimmed milk for 2 h at room temperature and incubated with antibody dilutions overnight at 4˚C using the following specific primary antibodies: VNN1 (1:1,000; cat. no. ab205912; Abcam), β-actin (1:1,000; cat. no. ab8227; Abcam), PPARγ (1:1,000; cat. no. ab209350; Abcam), tumor susceptibility gene 101 (TSG101; 1:1,000; cat. no. ab133586; Abcam), Alix (1:1,000; cat. no. ab275337; Abcam), C-myc (1:2,000; cat. no. ab185656; Abcam), pancreatic and duodenal homeobox 1 (Pdx1; 1:3,000; cat. no. ab47267; Abcam), neurogenic differentiation 1 (NeuroD1; 1:1,000; cat. no. ab109224; Abcam), glyceraldehyde 3-phosphate dehydrogenase (GAPDH; 1:2,500; cat. no. ab9485; Abcam), Lamin B (1:1,000; cat. no. ab16048; Abcam), Forkhead box protein O1 (FoxO1; 1:1,000; cat. no. ab52857; Abcam), cleaved caspase-3 (1:1,000; cat. no. 9664; Cell Signaling Technology, Inc.), cleaved caspase-9 (1:1,000; cat. no. 9509; Cell Signaling Technology, Inc.), MAF BZIP transcription factor A (Mafa; 1:1,000; cat. no. 79737; Cell Signaling Technology, Inc.), AMP-activated protein kinase (AMPK; 1:1,000; cat. no. 2532; Cell Signaling Technology, Inc.), phosphorylated (p-)AMPK (1:1,000; cat. no. 2535; Cell Signaling Technology, Inc.), tubulin (1:1,000; cat. no. 2146; Cell Signaling Technology, Inc.) and sirtuin 1 (Sirt1; 1:1,000; cat. no. 2028; Cell Signaling Technology, Inc.). The membranes were then incubated with anti-rabbit IgG (HRP-linked) secondary antibody (1:1,000; cat. no. 7074; Cell Signaling Technology, Inc.) for 1 h at room temperature. The protein bands were visualized using EZ-ECL (cat. no. 20-500-120; Biological Industries, Inc.). The bands were quantitated using ImageJ software (version 1.8.0; National Institutes of Health).

Insulin secretion assay. Following co-culture with PC cells or PC-Exos for 24 h, the islets were incubated in Krebs-Ringer bicarbonate buffer (KRBB) for 45 min. Subsequently, the medium was removed, and the islets were incubated in KRBB containing either 5.6 or 16.7 mM glucose for 30 min. The supernatants were collected following centrifugation at 1,000 x g for 5 min at 4˚C, and the islets were then dissociated into single cells and incubated overnight in acidified ethanol at 4˚C. The supernatants were then collected following centrifugation at 3,000 x g for 5 min at 4˚C. The insulin contents in all the supernatants were analyzed using the Insulin Radioimmunoassay kit (cat. no. S10930046; Beijing North Institute of Biotechnology Co., Ltd.). Total cell protein was determined using BCA assay for normalizing the insulin content measurements.

Determination of the cysteamine content using high-performance liquid chromatography (HPLC). The cysteamine contents in the conditioned media of PC cells and lysates of islets were determined using HPLC. The detailed procedures were performed according to standard protocols, as described in a previous study by the authors (11). The HPLC system was constructed using an ESA-model 542 pump and an ESA Coulochem III coulometric detector (Waters Corporation). The analysis voltage, current and output voltage of detector 1 (E1) were set at -150 mV, 10 nA and -1.00 V, respectively; the analysis voltage and current of detector 2 (E2) were set at +200 mV and 1 μA, respectively. The chromatographic column (Hypersil BDS C18 column, 250x4.6 mm I.D., 5 μM; Dalian Elite Analytical Instruments Co., Ltd.) was rinsed using a mixture of ultrapure water and acetonitrile overnight to remove salts or other impurities. The pH of the mobile phase (50 mM NaH_2PO_4, 0.05 mM octane sulfonic acid, 1% acetonitrile and 0.5% N,N-dimethylformamide) was adjusted to 2.52, and the mobile phase was then filtered using nylon filters with a pore size of 0.22 μm (MilliporeSigma). A 100 μl conditioned medium or islets lysate was mixed with an equal volume of perchloric acid, and the supernatants were then collected following centrifugation at 13,000 x g for 20 min at 4˚C, the supernatants were transferred to Amicon Ultra-0.5 3K centrifugal filters (cat. no. UFC5003BK; MilliporeSigma) and centrifuged at 8,000 x g for 20 min at 4˚C. The solutions in the lower tubes were used as samples to be tested. The flow rate of the mobile phase was 0.6 ml/min. A 20 μl standard sample of cysteamine (cat. no. 30070; MilliporeSigma) or the sample to be tested were loaded into the autosampler (Waters Corporation), respectively. EZStart software (version 7.2; Scientific Systems Inc.) was used to analyze chromatograms.

Measurement of reactive oxygen species (ROS) generation. Following co-culture with PC cells, the islets were dissociated into single cells and treated with 10 μM DCF-DA (ROS-specific fluorescent probe; cat. no. 35845; MilliporeSigma) for 30 min at 37˚C; the cells were then resuspended in ice-cold PBS for analysis using flow cytometry (FCM; FACSCanto™ II; BD Biosciences). The data were analyzed using FlowJo software (version 7.6; FlowJo LLC).

Detection of GSH concentration. Following co-culture with PC cells, the islets were lysed with 10 mM HCl, then mixed with 5% sulfosalicylic acid. The supernatants were collected following centrifugation at 8,000 x g for 10 min at 4˚C and GSH in the supernatants was detected using a Total Glutathione Quantification kit (cat. no. T419; Dojindo Laboratories, Inc.).

Co-immunoprecipitation (Co-IP). Following pre-treatment with PC-Exos, non-denaturing protein lysates of islets were prepared in Nonidet P40 (NP-40) lysis buffer (50 mM Tris-HCl, pH 7.5, 1% NP-40, 100 mM NaCl) supplemented with a complete protease inhibitor cocktail (cat. no. 11697498001; Roche Co., Ltd.). Protein lysates were incubated with Sirt1 primary antibody (1:50; cat. no. 2028; Cell Signaling Technology, Inc.) and negative control IgG (1:50; cat. no. 2729; Cell Signaling Technology, Inc.) at 4˚C for 12 h, and immunocomplexes were incubated with the Protein A/G Beads (cat. no. LSKMAGAG; MilliporeSigma) for 2 h at 4˚C. The beads were washed three times with lysis buffer and boiled for 5 min at 100˚C, and immunocomplexes were then separated by 10% SDS-PAGE and examined using western blot analysis. For detection of FoxO1 acetylation, islet lysates were incubated with acetylated-lysine antibody (1:100; cat. no. 9441; Cell Signaling Technology, Inc.) for 12 h at 4˚C, and the immunocomplexes were then examined using western blot analysis following incubation with FoxO1 antibody (1:1,000; cat. no. ab52857; Abcam) overnight at 4˚C.

Islet transplantation. As aforementioned, all animal experiments in the present study were approved by the Animal Ethics Committee of The First Affiliated Hospital of Zhengzhou University. A total of 40 B6 mice (female; 6 weeks old) were used as possible recipients for islet transplantation. These B6 mice were housed at 5 mice per cage under SPF conditions (temperature, 24˚C; humidity, 55%; 12-h light/dark cycle; free access to food and water). The B6 mice were rendered diabetic by an intraperitoneal injection of streptozotocin (180 mg/kg; cat. no. S0130; MilliporeSigma) 4-5 days prior to islet transplantation and the blood glucose levels of these mice were monitored using blood samples obtained from the tail vein. When two consecutive blood glucose levels were >18 mM, the B6 mice were confirmed as diabetic. A total of 30 B6 diabetic mice, which were active and had a good appetite, were selected as recipients and randomly divided into six groups (5 mice in each group). The other 10 B6 mice were euthanized by cervical dislocation following anesthesia by isoflurane inhalation (2-6% for induction; 1-3% for maintenance) 1 week later. The recipient mice were anaesthetized with isoflurane inhalation (2-6% for induction; 1-3% for maintenance). A 0.5-cm left subcostal incision was made to expose the left kidney. Subsequently, 200 or 400 IEQ islets treated or untreated with PC cells were transplanted under the left kidney capsule using a micromanipulator syringe. After the surgery, incisions were applied with 5% lidocaine cream (cat. no. H20063466; Beijing Ziguang Pharmaceutical Co., Ltd.) to alleviate the post-operative pain and the mice were placed in a warm environment until they were fully awake and had recovered from the anesthesia. The blood glucose levels of the recipients were monitored once a week. Blood glucose levels <10 mM was considered as normoglycemia. At the 14th week following islet transplantation, all recipient mice underwent a survival nephrectomy of the graft-bearing kidney using the same anesthesia and post-operative care methods as described above, and the blood glucose levels of these mice were then monitored. If the blood glucose levels increased significantly, this indicated that the normoglycemic levels of recipients were regulated by the transplanted islets under the kidney capsule.

When reaching one of the humane endpoints (>20% body weight loss, inability to eat, signs of immobility, abnormal posture, post-operative infection, post-operative hemorrhaging), the mice were euthanized. None of the mice reached the humane endpoints and died during the experimental procedures. Animal health and behavior were monitored daily. All recipient mice were euthanized by cervical dislocation with prior anesthesia by isoflurane inhalation (2-6% for induction; 1-3% for maintenance) at the 15th week following islet transplantation. Death was verified by the observation of pupil dilation, and by the cessation of respiration and heartbeat for 10 min.

Immunohistochemistry. The left kidneys of the recipients were resected at the 14th week following islet transplantation and fixed in zinc formalin fixative (cat. no. 3261477; MilliporeSigma) overnight at 4˚C, and then washed three times with 70% ethanol and embedded in paraffin. After the islets were incubated with PC-Exos for 24 h at 37˚C, the islets were fixed in zinc formalin fixative overnight at 4˚C and embedded in 1% agarose gel. The agarose gel-embedded tissue sections were incubated with VNN1 primary antibody (1:100; cat. no. ab205912; Abcam) overnight at 4˚C, and the paraffin-embedded tissue sections were incubated with insulin primary antibody (1:100; cat. no. 4590; Cell Signaling Technology, Inc.) overnight at 4˚C. Then biotin-labeled secondary antibody and streptavidin-peroxidase complex working solution (cat. no. SA1028; Boster Biological Technology Co., Ltd.) were incubated with the tissue sections for 1 h at 37˚C and a DAB kit (cat. no. AR1027; Boster Biological Technology Co., Ltd.) was used to produce a brown positive reaction. Finally, All sections were stained with hematoxylin (cat. no. C0105S-1; Beyotime Institute of Biotechnology) for 2 min at room temperature and eosin (cat. no. C0105S-2; Beyotime Institute of Biotechnology) for 30 sec at room temperature. Scans were performed and images were captured using a light microscope (Olympus IX-71; Olympus Corporation).

Statistical analysis. Statistical analysis was performed using SPSS software (version 19.0; IBM Corp.). Data are expressed as the mean ± standard deviation (SD). One-way analysis of variance (ANOVA) with a Tukey's post hoc test was used for multiple-group comparisons. $P<0.05$ was considered to indicate a statistically significant difference. Data visualization was performed using GraphPad Prism software (version 5.0; GraphPad Software, Inc.).

Results

VNN1 overexpressed in PC cells inhibits the viability and further impairs the functions of paraneoplastic islets. The PANC-1 and CFPAC-1 cells were transfected with VNN1 vector (PV and CV, respectively) or empty vector (PE and CE, respectively), and the transfection efficiency was verified using western blot analysis (Fig. 1A). VNN1 overexpression had no significant effect on the proliferation of the PANC-1 and CFPAC-1 cells (Fig. S1). Primary islets were isolated from the pancreases of B6 mice and cultured *in vitro* (Fig. 1B). The islets were then co-cultured with PC cells for 24 h using Transwell chambers (Fig. 1C). As shown in Fig. 1D, the survival rate of the islets was decreased significantly in the PV or CV co-culture group compared with the control groups. Furthermore, the levels of pro-apoptotic proteins (cleaved caspase-3/9) in the PV or CV co-cultured islets were increased significantly (Fig. 1E). Compared with the untreated group, the basal insulin secretion of islets markedly decreased in all co-culture groups, and the decrease was more pronounced in the PV co-culture group (Fig. 1F, left panel). Following low-glucose (5.6 mM) or high-glucose (16.7 mM) stimulation, the insulin secretion markedly increased in the PANC-1 and PE co-culture groups, while the insulin secretion exhibited no response in the PV co-culture group (Fig. 1F, left panel). Similar results were obtained for the CFPAC-1, CE and CV co-culture groups (Fig. 1F, right panel).

Inhibition of VNN1-mediated oxidative stress improves the viability and functions of paraneoplastic islets. The HPLC method was used (Fig. S2) to observe the cysteamine concentrations in the conditioned media of PV and CV cells; the cysteamine concentrations were increased significantly in the

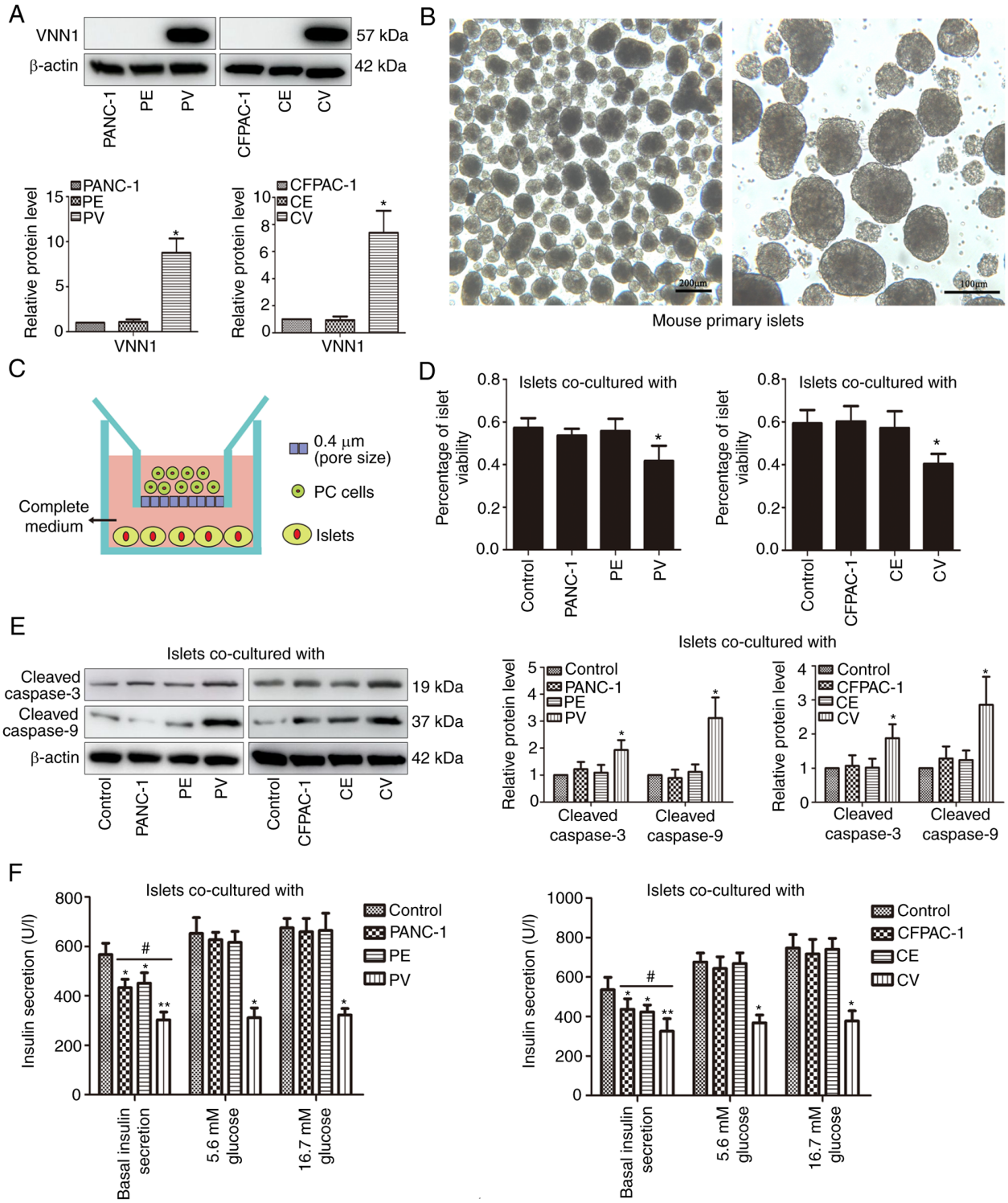

Figure 1. VNN1-overexpressing PC cells inhibit the viability and function of islets. (A) PANC-1 and CFPAC-1 cells were transfected with empty vector or VNN1 vector, and VNN1 expression in cell lysates was examined using western blot analysis. β-actin was used as the loading control. (B) Primary islets from B6 mice were cultured *in vitro*. (C) Co-culture system of islets with PC cells was constructed using Transwell chambers. (D) Following co-culture with PC cells for 24 h, islets were dissociated into single cells and cell viability was determined using Trypan blue staining. (E) Following co-culture with PC cells, cleaved caspase-3/9 expression levels in islets were examined using western blot analysis. β-actin was used as the loading control. (F) Following co-culture with PC cells, the insulin secretion of islets was determined using radioimmunoassay. Data are presented as the mean ± SD (n=3). Data were analyzed using one-way ANOVA followed by Tukey's post-hoc test. *P<0.05 and **P<0.01 compared with the PANC-1, CFPAC-1 or control group. $^{\#}$P<0.05 compared with the PANC-1, PE, CFPAC-1 or CE groups. VNN1, Vanin-1; PC, pancreatic cancer; PV, PANC-1 cells with the stable overexpression of VNN1; PE, PANC-1 cells transfected with empty vector; CV, CFPAC-1 cells with the stable overexpression of VNN1; CE, CFPAC-1 cells transfected with empty vector.

PV and CV cells compared with the control cells (Fig. 2A). Correspondingly, the cysteamine and ROS contents in the islets co-cultured with PV and CV cells were also markedly increased (Fig. 2B and C). In addition, the GSH and PPARγ expression levels in the islets were inhibited in the PV and CV co-culture groups (Fig. 2D and E). Following islet

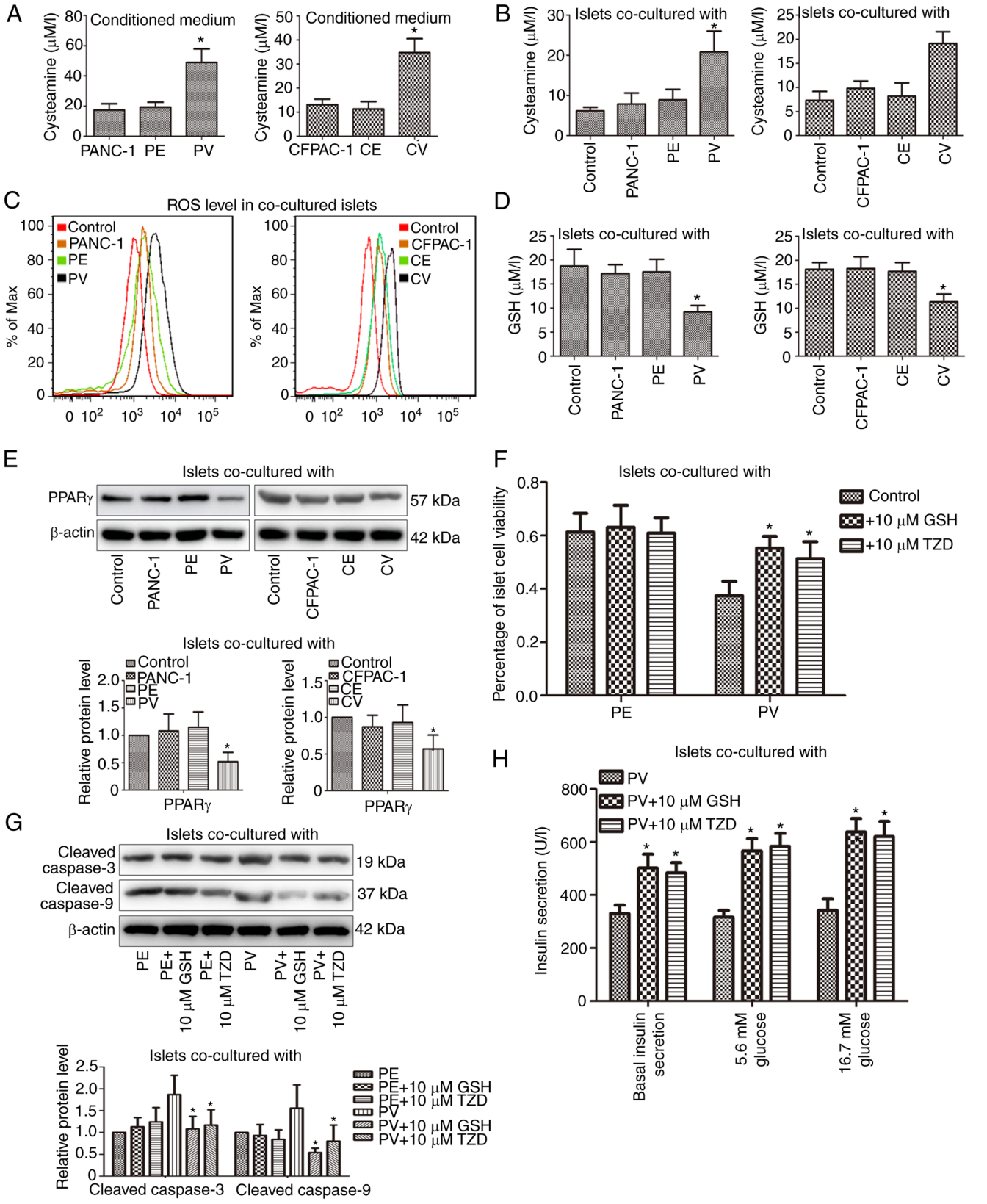

Figure 2. The viability and function of paraneoplastic islets are improved after suppressing VNN1-induced oxidative stress by GSH or TZD. (A and B) The extracellular and intracellular cysteamine concentrations were detected using high-performance liquid chromatography. (C) ROS contents in islets were analyzed using flow cytometry. (D) GSH concentrations in islets were detected using spectrophotometry. (E) PPARγ expression in islets was examined using western blot analysis. β-actin was used as the loading control. (F) Following islet pre-treatment with GSH or TZD, islet viability was determined using Trypan blue staining. (G) Following islet pre-treatment with GSH or TZD, cleaved caspase-3/9 levels in islets were examined using western blot analysis. β-actin was used as the loading control. (H) Following islet pre-treatment with GSH or TZD, the insulin secretion was determined using radioimmunoassay. Data are presented as the mean ± SD (n=3). Data were analyzed using one-way ANOVA followed by Tukey's post-hoc test. *P<0.05 compared with the PANC-1, CFPAC-1, PV or control group. ROS, reactive oxygen species; PPARγ, peroxisome proliferator activated receptor gamma; GSH, glutathione; TZD, thiazolidinedione; PV, PANC-1 cells with the stable overexpression of VNN1; PE, PANC-1 cells transfected with empty vector; CV, CFPAC-1 cells with the stable overexpression of VNN1; CE, CFPAC-1 cells transfected with empty vector; VNN1, Vanin-1.

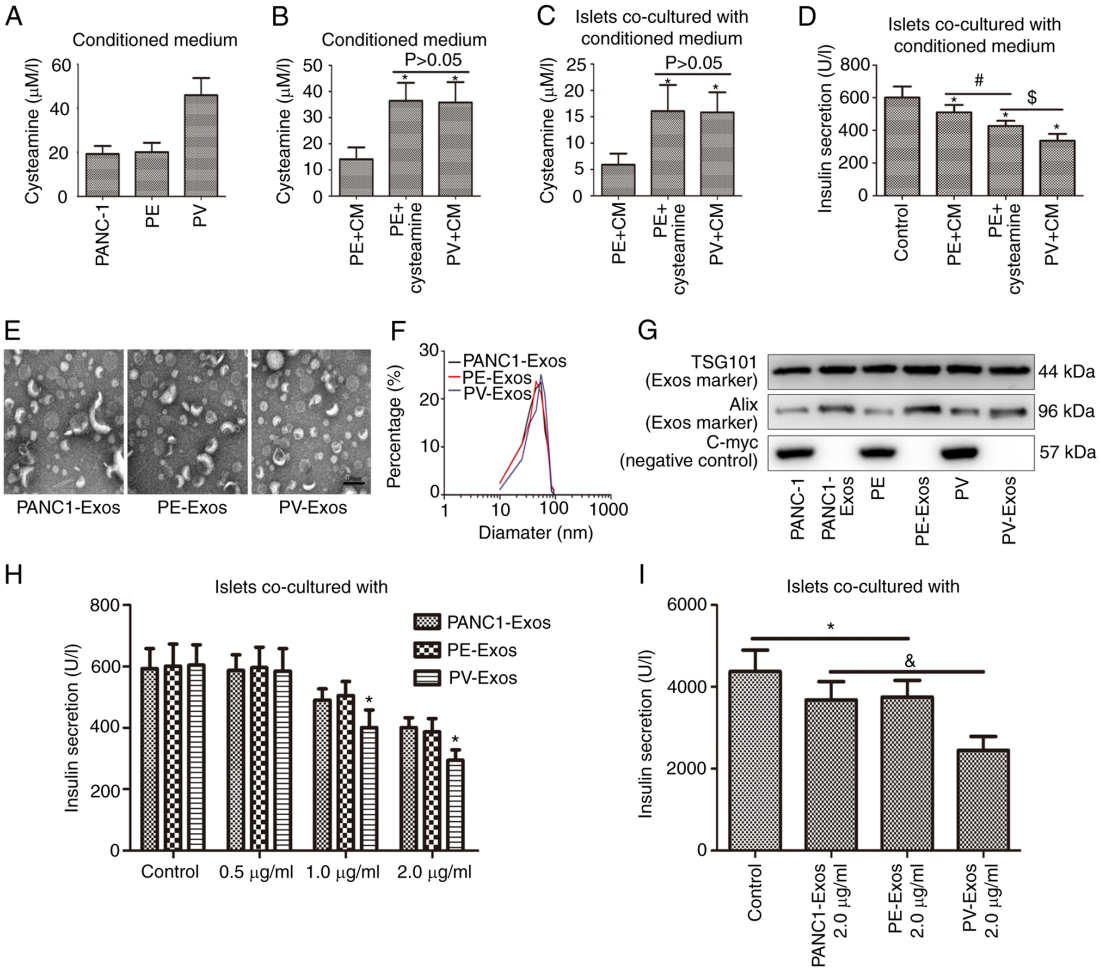

Figure 3. Islet dysfunction was exacerbated by Exos extracted from VNN1-overexpressing PC cells. (A and B) Cysteamine contents in conditioned media were determined using high-performance liquid chromatography. After the islets wereco-cultured with different conditioned media, (C) the cysteamine contents in islets were detected using high-performance liquid chromatography and (D) insulin secretion was determined using radioimmunoassay. (E) Transmission microcopy images of PC- Exos. (F) Size distributions of PC-Exos. (G) Exo markers (TSG101 and Alix) and negative marker (C-myc) in PC-Exos were determined using western blot analysis. TSG101 and Alix were used as the positive loading controls, and C-myc was used as the negative loading control. (H) Following treatment with different PC-Exos, the insulin secretion of islets was determined using radioimmunoassay. (I) Following treatment with different PC-Exos, the insulin content in islets was also determined using radioimmunoassay. Data are presented as the mean ± SD (n=3). Data were analyzed using one-way ANOVA followed by Tukey's post-hoc test. *P<0.05 compared with the PANC-1, PE + CM, PANC1-Exos or control group. #P<0.05 compared with the PE + CM group. $P<0.05 compared with the PE + cysteamine group. &P<0.05 compared with the PANC1-Exos or PE-Exos group. CM, complete medium; Exos, exosomes; VNN1, Vanin-1; PC, pancreatic cancer; PV, PANC-1 cells with the stable overexpression of VNN1; TSG101, tumor susceptibility gene 101; PE, PANC-1 cells transfected with empty vector.

pre-incubation with 10 μM GSH or 10 μM thiazolidinedione (TZD, PPARγ agonist) for 2 h, the decreased survival rate and increased expression levels of pro-apoptotic proteins in the islets were reversed in the PV co-culture group (Fig. 2F and G). Moreover, following islet pre-treatment with GSH or TZD for 2 h, the basal insulin secretion was increased significantly and the insulin secretion was also markedly elevated following low- or high-glucose stimulation in the PV co-culture group (Fig. 2H).

Exos derived from PV cells further suppress the insulin secretion of paraneoplastic islets. As was demonstrated, the cysteamine concentration in the conditioned medium of PV cells was higher than that of the control cells (Fig. 3A). In order to ensure that the conditioned media of PE and PV cells contain the same content of cysteamine, the difference value (D-value) of cysteamine content between the two types of conditioned media was calculated, and complete medium (CM) containing the standard sample of cysteamine (the amount was equal to the D-value) was mixed with conditioned medium of PE cells (PE + cysteamine), and the equal volume of CM without cysteamine was mixed with conditioned medium of PE cells (PE + CM) or PV cells (PV + CM), respectively. As shown in Fig. 3B, the cysteamine concentration in the conditioned medium of the PE + cysteamine group was equal to that of the PV + CM group. Following islet incubation with the different conditioned media for 24 h, the cysteamine content in the islets exhibited no marked differences between the PE + cysteamine and PV + CM groups (Fig. 3C). Although the insulin secretion of islets was inhibited in both the PE + cysteamine and PV + CM groups, the inhibitory effect was more prominent in the PV + CM group (Fig. 3D), which indicated that other unknown substances released by VNN1-overexpressing PC cells may also aggravate islet dysfunction, apart from cysteamine.

Transmission electron microscopy images revealed that the morphologies of extracellular vesicles (EVs) extracted

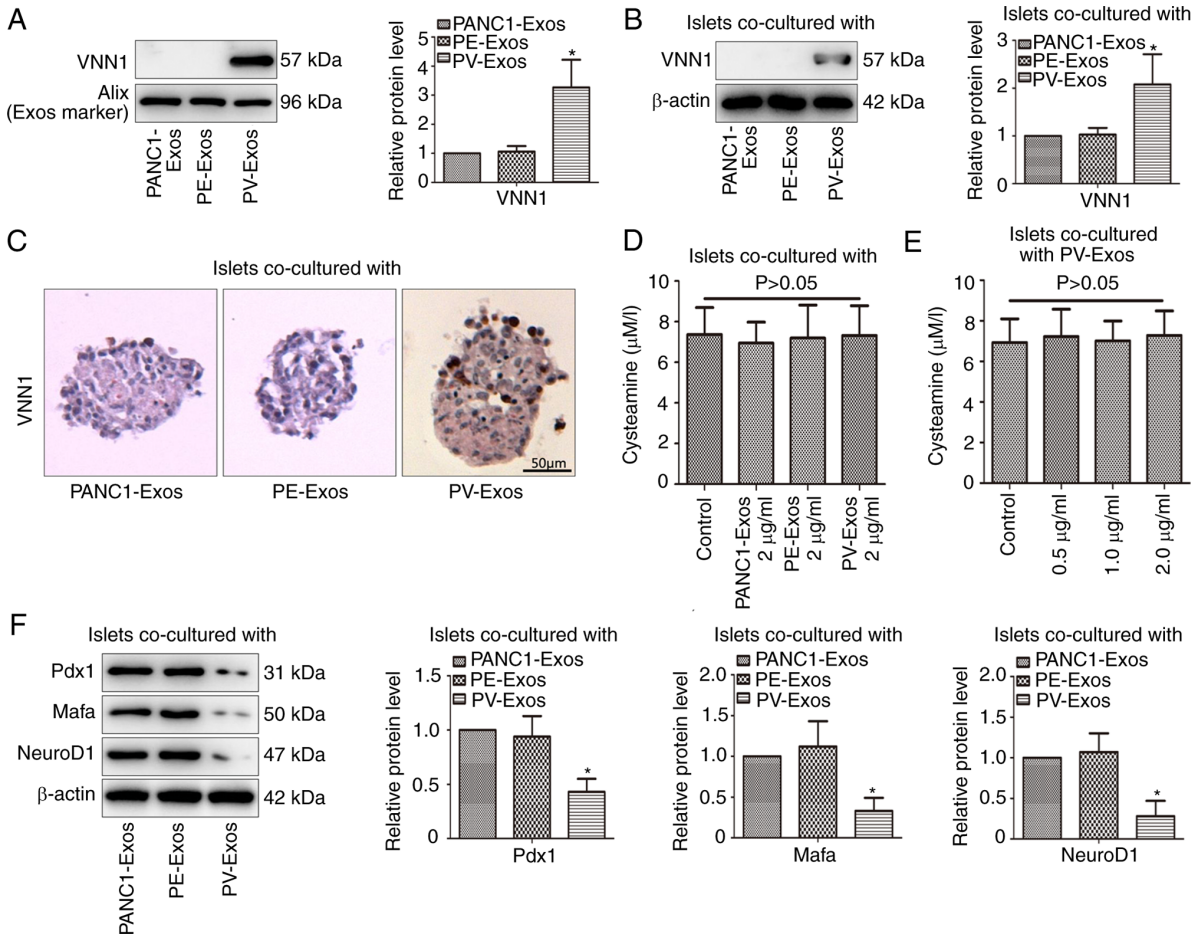

Figure 4. Exos derived from VNN1-overexpressing PC cells induce β-cell dedifferentiation. (A) VNN1 in PC-Exos was determined using western blot analysis. As an Exo marker, Alix was used as the loading control. (B) Following treatment with PC-Exos, VNN1 expression in islets was determined using western blot analysis. β-actin was used as the loading control. Following co-culture with PC-Exos, (C) VNN1 expression in islets was analyzed using immunohistochemistry, and (D) cysteamine in islets was determined using high-performance liquid chromatography. (E) Following incubation with various concentrations of PV-Exos, cysteamine in islets was determined using high-performance liquid chromatography. (F) Following co-culture with PC-Exos, β-cell differentiation markers (Pdx1, Mafa and NeuroD1) in islets were examined using western blot analysis. β-actin was used as the loading control. Data are presented as the mean ± SD (n=3). Data were analyzed using one-way ANOVA followed by Tukey's post-hoc test. *P<0.05 compared with the PANC1-Exos group. VNN1, Vanin-1; Exos, exosomes; Pdx1, pancreatic and duodenal homeobox 1; Mafa, MAF BZIP transcription factor A; NeuroD1, neurogenic differentiation 1; PC, pancreatic cancer; PV, PANC-1 cells with the stable overexpression of VNN1; PE, PANC-1 cells transfected with empty vector.

from PC cells were diverse (Fig. 3E), and the particle sizes of the EVs ranged from 30 to 80 nm (Fig. 3F). All EVs contained Exo-specific proteins (TSG101 and Alix), apart from C-myc, which was confirmed not to be expressed in Exos (Fig. 3G). Therefore, the extracted EVs were Exos. The islets were incubated with types of Exos (PANC1-Exos, PE-Exos and PV-Exos) for 24 h. Compared with the untreated group, the insulin secretion of islets in the PC-Exo-treated groups were markedly decreased as the concentration of Exos increased, and the decrease was particularly evident in the PV-Exo-treated group (Fig. 3H). After the islets were incubated with 2 μg/ml of PC-Exos for 24 h, the insulin content in the islets decreased in every PC-Exo-treated group, and the decrease was particularly pronounced in the PV-Exo-treated group (Fig. 3I).

VNN1 can be transferred into paraneoplastic islets through PC-Exos and induces β-cell dedifferentiation. As shown in Fig. 4A, VNN1 expression in PV-Exos was higher than that in PANC1-Exos and PE-Exos. After the islets were incubated with PC-Exos (2 μg/ml) for 24 h, the VNN1 content in the PV-Exo-treated islets was also higher than that in the PANC1-Exos and PE-Exo-treated islets (Fig. 4B and C). These results suggested that VNN1 could be transferred into islets via PC-Exos. Notably, there was no marked difference in the cysteamine content among these three PC-Exo-treated islets (Fig. 4D). The islets were incubated with various concentrations of PV-Exos for 24 h, and no marked changes were observed in the cysteamine content of islets with the increased concentration of PV-Exos (Fig. 4E). These results demonstrated that the further inhibition of islet function by PV-Exos was not dependent on cysteamine-mediated oxidative stress. Therefore, the present study continued to explore the mechanisms of the PV-Exo-induced aggravation of islet dysfunction. Compared with the PANC1-Exos and PE-Exos, the PV-Exos significantly decreased the expression of β-cell differentiation markers (Pdx1, Mafa and NeuroD1) in the islets (Fig. 4F), which indicated that PV-Exos induced β-cell dedifferentiation.

VNN1 in PC-Exos induce β-cell dedifferentiation via the inhibition of the AMPK/GAPDH/Sirt1/FoxO1 signaling pathway.

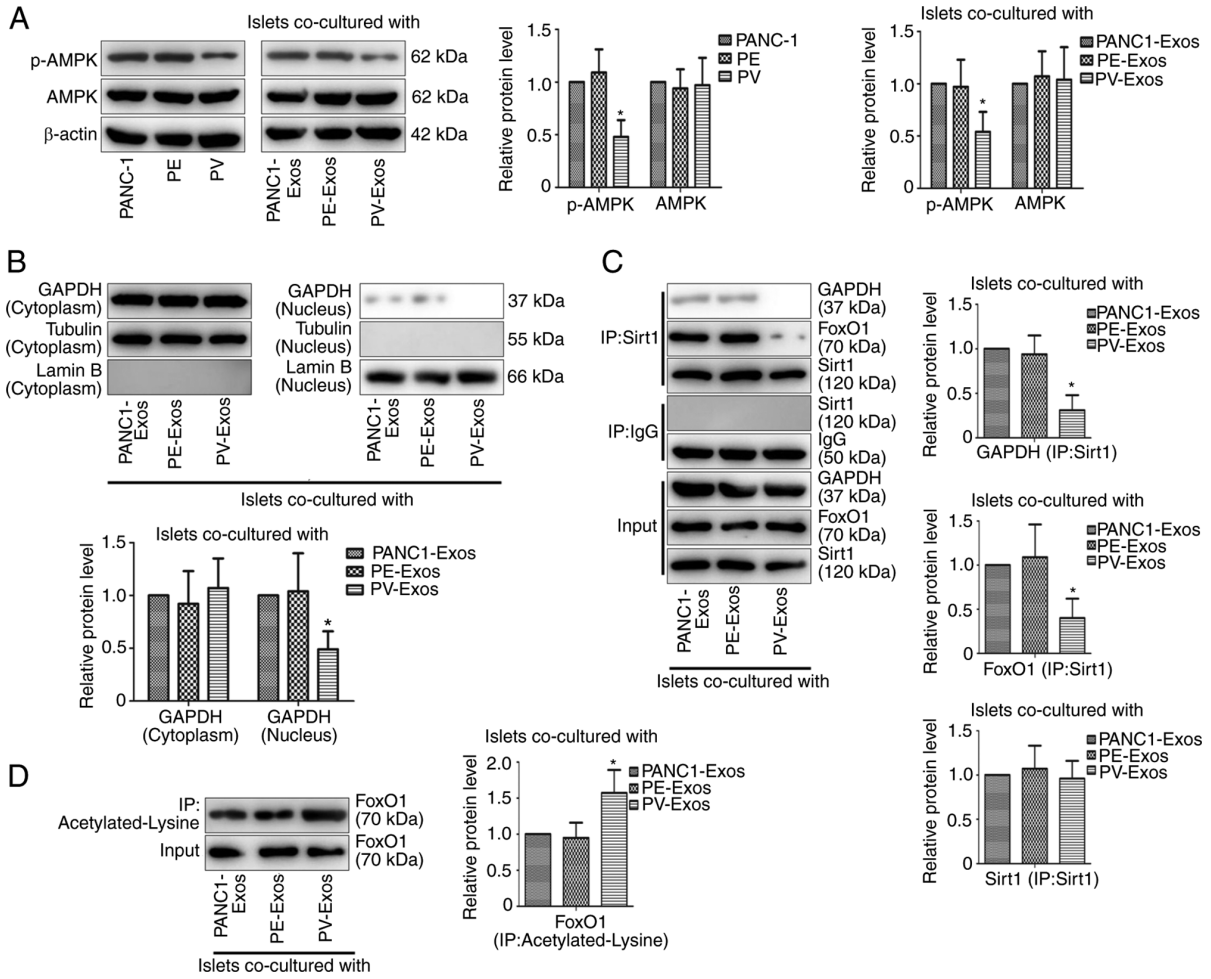

Figure 5. VNN1 in PC-Exos inhibits the AMPK/GAPDH/Sirt1/FoxO1 signaling pathway in islets. (A, left panel) p-AMPK levels in PC cells were determined using western blot analysis. β-actin was used as the loading control. (A, right panel) Following treatment with PC-Exos, p-AMPK levels in islets were examined using western blot analysis. β-actin was used as the loading control. (B) Following treatment with PC-Exos, nuclear-localized GAPDH in islets were examined using western blot analysis. Tubulin and Lamin B were used as the loading controls. (C) Following co-culture with PC-Exos, the interaction of GAPDH or FoxO1 with Sirt1 in islets was detected using co-immunoprecipitation. GAPDH, FoxO1 and Sirt1 were used as the loading controls. (D) Following co-culture with PC-Exos, acetylated-lysine of FoxO1 in islets was detected using co-immunoprecipitation. FoxO1 was used as the loading control. Data are presented as the mean ± SD (n=3). Data were analyzed using one-way ANOVA followed by Tukey's post-hoc test. *P<0.05 compared with the PANC-1 or PANC1-Exos group. p-, phosphorylated; Exos, exosomes; VNN1, Vanin-1; AMPK, AMP-activated protein kinase; PC, pancreatic cancer; PV, PANC-1 cells with the stable overexpression of VNN1; PE, PANC-1 cells transfected with empty vector.

The present study attempted to investigate the mechanisms of PV-Exo-induced β-cell dedifferentiation. It was found that VNN1 overexpression inhibited the phosphorylation of AMPK in PANC-1 cells, and the expression of p-AMPK in the PV-Exo-treated islets was lower than that in the PANC1-Exos and PE-Exo-treated islets (Fig. 5A), suggesting that VNN1 transferred by PC-Exos inhibited the phosphorylation of AMPK in paraneoplastic islets. The present study further examined the effects of PV-Exos on downstream cytokines of the AMPK signaling pathway in islets. Compared with the control groups, the content of GAPDH was decreased in the nucleus of PV-Exo-treated islets (Fig. 5B). A Co-IP assay was also performed to confirm that Sirt1 could bind with GAPDH and FoxO1 in PC-Exo-treated islets, while the bindings were inhibited in PV-Exo-treated islets (Fig. 5C). In addition, Co-IP assay revealed that lysine of FoxO1 was markedly acetylated in the PV-Exo-treated islets (Fig. 5D), indicating that PV-Exos suppressed FoxO1 deacetylation in islets. As FoxO1 functions as a downstream protein of the AMPK/GAPDH/Sirt1 signaling pathway and FoxO1 deacetylation induces β-cell differentiation, these results suggested that VNN1 in PC-Exos inhibited the AMPK/GAPDH/Sirt1/FoxO1 signaling pathway to induce β-cell dedifferentiation.

Co-culture with PV cells aggravates the dysfunction of islets transplanted under the kidney capsule of diabetic mice. Islets were co-cultured with PE and PV cells for 24 h, and these islets and untreated islets were then transplanted under the kidney capsule of B6 diabetic mice. As shown in Fig. 6A, the mice that received 200 IEQ untreated islets achieved normoglycemia at the 2nd week post-transplantation, and the mice that received the same amount of PE or PV cell-treated islets achieved normoglycemia at the 4th or 6th week post-transplantation, respectively. The fasting blood glucose (FBG) levels of the untreated group were lower at the 1st to 3rd weeks post-transplantation compared to the PE and PV groups. The FBG levels of the PV group were higher at the 2nd to 4th weeks post-transplantation compared to the PE group.

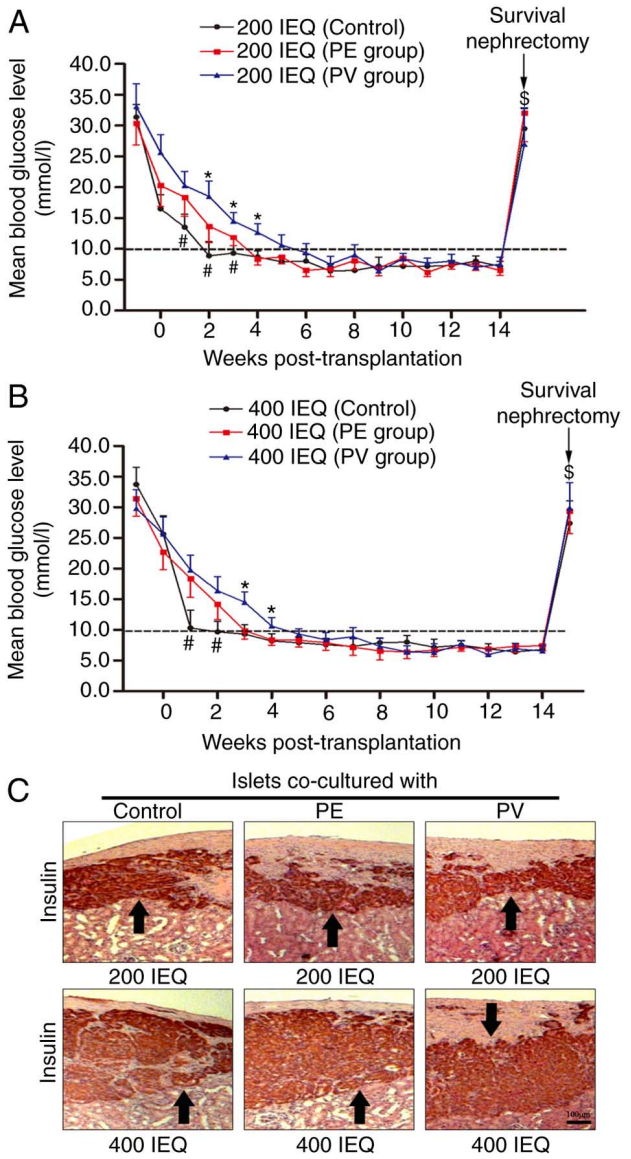

Figure 6. Secretions of VNN1-overexpressing PC cells aggravate islet dysfunction *in vivo*. (A and B) Average blood glucose levels of B6 diabetic mice before and after transplantation with 200 or 400 IEQ islets co-cultured or not with PC cells under the kidney capsule (5 mice in each group). (C) Immunohistochemical analysis of insulin in islets under the kidney capsule (indicated with black arrows). Data are presented as the mean ± SD (n=5). Data were analyzed using one-way ANOVA followed by Tukey's post-hoc test. *P<0.05, PV group compared with the PE group; $^{\#}$P<0.05, untreated group compared with the PE or PV group; $^{\$}$P<0.05 compared with untreated, PE or PV group at 14th week. IEQ, islet equivalent; VNN1, Vanin-1; PV, PANC-1 cells with the stable overexpression of VNN1; PE, PANC-1 cells transfected with empty vector.

Similar results were observed for the mice which received 400 IEQ islets. As shown in Fig. 6B, mice in the untreated, PE and PV groups achieved normoglycemia at the 2nd, 3rd and 5th week post-transplantation, respectively. The FBG levels in the untreated group were lower at the 1st to 2nd weeks post-transplantation compared to the PE and PV groups. The FBG levels in the PV group were higher at the 3rd to 4th weeks post-transplantation compared to the PE group. Following the excision of kidney containing the transplanted islets at the 14th week, the FBG levels of all mice rebounded significantly (Fig. 6A and B), indicating that the transplanted islets were responsible for maintaining normoglycemia prior to nephrectomy. The excised kidneys were used for immunohistochemical staining, and the islets stained positive for insulin could be observed under the kidney capsule (Fig. 6C).

Discussion

VNN1 can regulate the oxidative stress response via multiple pathways (9,20-22). In addition, oxidative stress can impair the activity and function of β-cells by damaging molecules or organelles, which leads to the onset and development of diabetes (23-26). In a previous study, the authors found that the high expression of VNN1 in PC cells aggravated the oxidative stress of paraneoplastic insulinoma cell lines by paracrine cysteamine, thereby inhibiting the activity and function of insulinoma cells (11). Cell lines derived from tumor cells differ from normal cells in terms of gene expression, metabolic pathways, growth patterns, etc. Therefore, primary mouse islets were used in the present study in order to obtain more accurate research results. As the paracrine effect of PC cells is likely to induce islet dysfunction (27-29), the primary islets were co-cultured with PC cells *in vitro* to simulate the paracrine effect of PC cells on paraneoplastic islets *in vivo* in the present study. Consistent with the findings of the previous study by the authors (11), the present study also found that VNN1-overexpressing PC cells increased the ROS levels, and decreased the GSH and PPARγ concentrations in paraneoplastic islets by secreting cysteamine, and subsequently aggravated oxidative stress in islets, ultimately inhibiting the viability and insulin secretion of islets (Fig. S3).

In the present study, it was found that other substances secreted by VNN1-overexpressing PC cells also further inhibited the function of paraneoplastic islets in addition to cysteamine. Some studies have indicated that PC-Exos may induce the occurrence of PC-DM. Javeed *et al* (13) demonstrated that adrenomedullin in PC-Exos inhibited the insulin secretion of β-cells by inducing endoplasmic reticulum stress. Moreover, adrenomedullin in PC-Exos also leads to lipolysis, which produces free fatty acids to impair insulin secretion and induce insulin resistance (15,17). Wang *et al* (14) found that microRNAs (miRNAs/miRs; e.g., miR-883b-5p, etc.) in PC-Exos triggered the insulin resistance of skeletal muscle cells. Zhang *et al* (16) observed that miRNAs (miR-6796-3p, etc.) in PC-Exos decreased the expression of incretins in enteroendocrine cells, thereby inhibiting insulin secretion and reducing insulin sensitivity. The present study found that PC-Exos (1 or 2 μg/ml) inhibited the insulin secretion of islets, and the inhibitory effect of VNN1-overexpressing PC-Exos was more prominent. In addition, it was found that VNN1 could be transferred into paraneoplastic islets via PC-Exos. However, there was no significant difference in the cysteamine content in islets following incubation with PC-Exos (≤2 μg/ml), regardless of whether VNN1 was overexpressed in PC cells. This indicated that the further inhibition of islet function by VNN1-overexpressing PC-Exos was not dependent on cysteamine-mediated oxidative stress.

Previous studies have suggested that β-cell apoptosis caused by oxidative stress is the primary etiology of diabetes which results in the decrease in the number and dysfunction of β-cells (30,31). However, other researchers have found

that the decrease in the number and dysfunction of β-cells is not proportional to the degree of β-cell apoptosis, indicating that other mechanisms may also inhibit the activity and function of β-cells besides apoptosis (32). Cell dedifferentiation refers to the transformation of functionally mature cells into more primitive precursor cells after losing their specific phenotype and function. Recent research has reported that dedifferentiated β-cells lose their ability to secrete insulin and transform into endocrine precursor cells with pluripotent differentiation potential, resulting in the insufficiency in quantity and function of β-cells (33). Therefore, β-cell dedifferentiation may be another key mechanism in the pathogenesis of diabetes.

Chang *et al* (34) found that cytoplasmic GAPDH can be phosphorylated by activated AMPK, which causes GAPDH to redistribute into the nucleus, and nuclear-localized GAPDH then interacts directly with Sirt1 and disassociates Sirt1 from its inhibitor, deleted in breast cancer 1 (DBC1), thereby causing Sirt1 to be activated. Nakae *et al* (35) observed that activated Sirt1 could bind directly with FoxO1 and induce the deacetylation of FoxO1, thereby increasing the transcriptional activity of FoxO1. Some studies have confirmed that the increased transcriptional activity of FoxO1 can promote the expression of β-cell differentiation markers, such as Mafa and NeuroD1, while the decreased transcriptional activity of FoxO1 induces β-cell dedifferentiation (36-38). The present study demonstrated that VNN1-overexpressing PC-Exos inhibited the expression of β-cell differentiation markers (Pdx1, Mafa and NeuroD1) in islets. It was also found that VNN1 inhibited the phosphorylation of AMPK in islets via PC-Exos. The present study observed that the GAPDH content was decreased in the nucleus of islets following incubation with VNN1-overexpressing PC-Exos, suggesting that VNN1 inhibited the redistribution of GAPDH from the cytoplasm to the nucleus in islets. Moreover, the present study demonstrated that VNN1-overexpressing PC-Exos inhibited the binding of Sirt1 with GAPDH and FoxO1 in islets. As previously demonstrated, three lysine sites (Lys242, Lys245 and Lys262) of FoxO1 can be acetylated by lysine acetylation transferases, resulting in the acetylation of FoxO1 (39). The present study found that the acetylated lysine level of FoxO1 in islets was upregulated following incubation with VNN1-overexpressing PC-Exos, suggesting that VNN1 in PC-Exos may promote the acetylation of FoxO1. In other words, VNN1 inhibited FoxO1 deacetylation in islets.

As summarized in Fig. 7, the possible mechanisms responsible for the dedifferentiation of paraneoplastic β-cells by VNN1-overexpressing PC-Exos are the following: i) VNN1 located in the PC cell membrane is acquired and enriched by PC-Exos; ii) PC-Exos are captured by paraneoplastic β-cells, and enriched VNN1 is transferred into β-cells; iii) VNN1 inhibits the phosphorylation of AMPK, thereby blocking the phosphorylation of GAPDH; iv) GAPDH is prevented from moving into the nucleus and binding with Sirt1, thereby limiting the disassociation of Sirt1 from its inhibitor, DBC1, resulting in a decrease in Sirt1 activity; v) inactivated Sirt1 cannot interact with FoxO1 and thus FoxO1 cannot be deacetylated, causing a decrease in the transcriptional activity of FoxO1; vi) β-cell dedifferentiation is initiated thereof.

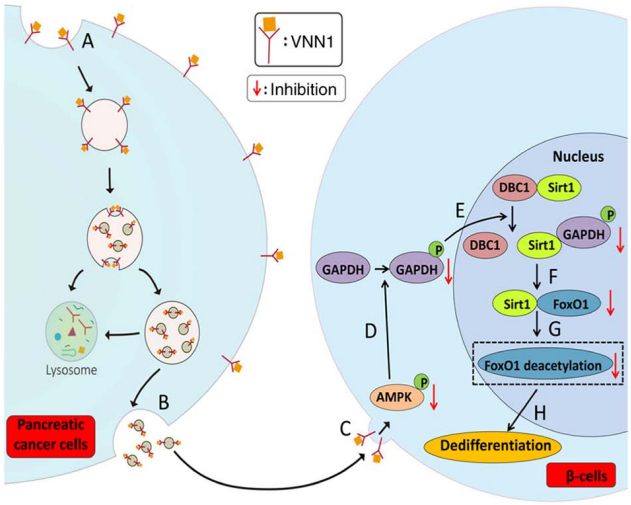

Figure 7. Schematic diagram illustrating the mechanisms through which VNN1 in PC cells induces β-cell dedifferentiation by inhibiting the AMPK/GAPDH/Sirt1/FoxO1 signaling pathway. (A) PC cell membrane acquires VNN1 by endocytosis and forms a small vesicle. (B) The multivesicular body fuses with the PC cell membrane and releases VNN1-containing Exos. (C) VNN1 is transferred into β-cells by PC-Exos and inhibits the phosphorylation of AMPK. (D) The phosphorylation of cytoplasmic GAPDH is inhibited by inactivated AMPK. (E) GAPDH is prevented from redistributing into the nucleus and interacting with Sirt1; hence, Sirt1 activity is inhibited. (F) Sirt1 is prevented from binding with FoxO1. (G) FoxO1 cannot be deacetylated. (H) β-cell dedifferentiation is initiated thereof. PC, pancreatic cancer; VNN1, Vanin-1; AMPK, AMP-activated protein kinase; FoxO1, Forkhead box protein O1; Sirt1, sirtuin 1.

A previous study reported that the blood glucose levels of SCID mice were evidently increased after a continuous intraperitoneal injection of conditioned medium of PC cells for 10 days (29). In addition, in another study, the blood glucose levels of athymic nude mice were significantly increased after an injection of PC cells subcutaneously and orthotopically at 4 weeks (40). However, these studies have not confirmed which cells are targeted by PC cells to cause hyperglycemia *in vivo*. *In vitro* experiments have demonstrated that the secretions of PC cells can impair the functions of β-cells, adipocytes, hepatocytes, skeletal muscle cells and enteroendocrine cells, all of which participate in the regulation of blood glucose *in vivo* (13-17,41). In the present study, to investigate the effects of islets following co-culture with PC cells on blood glucose regulation *in vivo* and to exclude the effects of the PC cell-induced dysfunction of other target cells on blood glucose regulation, B6 diabetic mice with islets transplanted under the kidney capsule were used. It was found that mice transplanted with 200 or 400 IEQ untreated islets achieved normoglycemia earlier than the mice transplanted with islets co-cultured with PC cells, while mice transplanted with islets treated with VNN1-overexpressing PC cells achieved normoglycemia at the latest stage. These results indicate that the secretions of PC cells can impair the functions of islets *in vivo*, and the secretions of VNN1-overexpressing PC cells aggravate islet dysfuntion. However, whether transplanted islets were co-cultured with PC cells or not, all mice achieved normoglycemia eventually, which may be caused by the following two reasons: i) The co-culture time of islets with PC cells

was brief, and the secretions of PC cells could not function continuously on transplanted islets; ii) the quantity of transplanted islets was sufficient.

Previous reports have demonstrated that VNN1 overexpression in colorectal or adrenocortical cancer promotes tumor progression and is associated with a poor prognosis (42-44). However, the effects of VNN1 on PC progression remain unknown. In the present study, it was found that VNN1 inhibited the phosphorylation of AMPK in PC cells. As activated AMPK can suppress the invasion and migration of PC cells (45,46), it was hypothesized that VNN1 may promote PC progression by inhibiting AMPK signaling pathway. Therefore, it may be noteworthy to investigate the role of VNN1 in PC progression and develop potential VNN1-targeted therapies for PC in the future.

In conclusion, the present study re-affirmed that VNN1 in PC cells aggravated oxidative stress in paraneoplastic islets by secreting cysteamine, thereby inhibiting the activity and function of islets. In addition, it was found that VNN1 was transferred into islets via PC-Exos and inhibited the AMPK/GAPDH/Sirt1/FoxO1 signaling pathway, resulting in β-cell dedifferentiation. Furthermore, a renal subcapsular islet transplantation model was used to demonstrate that the secretions of VNN1-overexpressing PC cells aggravated islet dysfunction *in vivo*. Therefore, the present study further explored the mechanisms of VNN1-induced PCAD and provide new evidence that VNN1 can be used as a specific biomarker for early PCAD screening.

Acknowledgements

Not applicable.

Funding

The present study was supported by grants from the National Natural Science Foundation of China (nos. 81301889 and 81700682), the Natural Science Foundation of Zhejiang Province (no. LY19H160042) and the Youth Innovation Fund Project of the First Affiliated Hospital of Zhengzhou University (no. 215709).

Availability of data and materials

The datasets used and/or analyzed during this study are available from the corresponding author on reasonable request.

Authors' contributions

WQ and MK designed the study. WQ, MK and CL performed the experiments. WQ, MK, CL, WZ and QG analyzed the statistical data, and assembled and installed the figures. WQ and MK supervised the study and confirm the authenticity of all the raw data. WQ wrote the manuscript. All authors have read and approved the final version of the manuscript.

Ethics approval and consent to participate

The animal experiments were approved by the Ethics Committee of The First Affiliated Hospital of Zhengzhou University (Ethics no. 2018-03-003; Zhengzhou, China).

Patient consent for publication

Not applicable.

Competing interests

The authors declare that they have no competing interests.

References

1. Cai J, Chen H, Lu M, Zhang Y, Lu B, You L, Zhang T, Dai M and Zhao Y: Advances in the epidemiology of pancreatic cancer: Trends, risk factors, screening, and prognosis. Cancer Lett 520: 1-11, 2021.
2. Sinha V, Shinde S, Saxena S, Thakur S, Walia T, Dixit V, Tiwari AK, Vishvakarma NK, Dwivedi M and Shukla D: A comprehensive review of diagnostic and therapeutic strategies for the management of pancreatic cancer. Crit Rev Oncog 25: 381-404, 2020.
3. Pannala R, Basu A, Petersen GM and Chari ST: New-onset diabetes: A potential clue to the early diagnosis of pancreatic cancer. Lancet Oncol 10: 88-95, 2009.
4. Pelaez-Luna M, Takahashi N, Fletcher JG and Chari ST: Resectability of presymptomatic pancreatic cancer and its relationship to onset of diabetes: A retrospective review of CT scans and fasting glucose values prior to diagnosis. Am J Gastroenterol 102: 2157-2163, 2007.
5. Boursi B, Finkelman B, Giantonio BJ, Haynes K, Rustgi AK, Rhim AD, Mamtani R and Yang YX: A clinical prediction model to assess risk for pancreatic cancer among patients with new-onset diabetes. Gastroenterology 152: 840-850.e3, 2017.
6. Aurrand-Lions M, Galland F, Bazin H, Zakharyev VM, Imhof BA and Naquet P: Vanin-1, a novel GPI-linked perivascular molecule involved in thymus homing. Immunity 5: 391-405, 1996.
7. Martin F, Malergue F, Pitari G, Philippe JM, Philips S, Chabret C, Granjeaud S, Mattei MG, Mungall AJ, Naquet P, *et al*: Vanin genes are clustered (human 6q22-24 and mouse 10A2B1) and encode isoforms of pantetheinase ectoenzymes. Immunogenetics 53: 296-306, 2001.
8. Pitari G, Malergue F, Martin F, Philippe JM, Massucci MT, Chabret C, Maras B, Duprè S, Naquet P and Galland F: Pantetheinase activity of membrane-bound Vanin-1: Lack of free cysteamine in tissues of Vanin-1 deficient mice. FEBS Lett 483: 149-154, 2000.
9. Dammanahalli KJ, Stevens S and Terkeltaub R: Vanin-1 pantetheinase drives smooth muscle cell activation in post-arterial injury neointimal hyperplasia. PLoS One 7: e39106, 2012.
10. Huang H, Dong X, Kang MX, Xu B, Chen Y, Zhang B, Chen J, Xie QP and Wu YL: Novel blood biomarkers of pancreatic cancer-associated diabetes mellitus identified by peripheral blood-based gene expression profiles. Am J Gastroenterol 105: 1661-1669, 2010.
11. Kang M, Qin W, Buya M, Dong X, Zheng W, Lu W, Chen J, Guo Q and Wu Y: VNN1, a potential biomarker for pancreatic cancer-associated new-onset diabetes, aggravates paraneoplastic islet dysfunction by increasing oxidative stress. Cancer Lett 373: 241-250, 2016.
12. Milane L, Singh A, Mattheolabakis G, Suresh M and Amiji MM: Exosome mediated communication within the tumor microenvironment. J Control Release 219: 278-294, 2015.
13. Javeed N, Sagar G, Dutta SK, Smyrk TC, Lau JS, Bhattacharya S, Truty M, Petersen GM, Kaufman RJ, Chari ST and Mukhopadhyay D: Pancreatic cancer-derived exosomes cause paraneoplastic β-cell dysfunction. Clin Cancer Res 21: 1722-1733, 2015.
14. Wang L, Zhang B, Zheng W, Kang M, Chen Q, Qin W, Li C, Zhang Y, Shao Y and Wu Y: Exosomes derived from pancreatic cancer cells induce insulin resistance in C2C12 myotube cells through the PI3K/Akt/FoxO1 pathway. Sci Rep 7: 5384, 2017.
15. Sagar G, Sah RP, Javeed N, Dutta SK, Smyrk TC, Lau JS, Giorgadze N, Tchkonia T, Kirkland JL, Chari ST and Mukhopadhyay D: Pathogenesis of pancreatic cancer exosome-induced lipolysis in adipose tissue. Gut 65: 1165-1174, 2016.
16. Zhang Y, Huang S, Li P, Chen Q, Li Y, Zhou Y, Wang L, Kang M, Zhang B, Yang B, *et al*: Pancreatic cancer-derived exosomes suppress the production of GIP and GLP-1 from STC-1cells in vitro by down-regulating the PCSK1/3. Cancer Lett 431: 190-200, 2018.

17. Sah RP, Nagpal SJ, Mukhopadhyay D and Chari ST: New insights into pancreatic cancer-induced paraneoplastic diabetes. Nat Rev Gastroenterol Hepatol 10: 423-433, 2013.
18. Cai H, Yang B, Xu Z, Zhang B, Xu B, Li X, Wu P, Chen K, Rajotte RV, Wu Y and Rayat GR: Cyanidin-3-O-glucoside enhanced the function of syngeneic mouse islets transplanted under the kidney capsule or into the portal vein. Transplantation 99: 508-514, 2015.
19. Rayat GR, Gazda LS, Hawthorne WJ, Hering BJ, Hosking P, Matsumoto S and Rajotte RV: First update of the international xenotransplantation association consensus statement on conditions for undertaking clinical trials of porcine islet products in type 1 diabetes-chapter 3: Porcine islet product manufacturing and release testing criteria. Xenotransplantation 23: 38-45, 2016.
20. Berruyer C, Martin FM, Castellano R, Macone A, Malergue F, Garrido-Urbani S, Millet V, Imbert J, Duprè S, Pitari G, *et al*: Vanin-1-/- mice exhibit a glutathione-mediated tissue resistance to oxidative stress. Mol Cell Biol 24: 7214-7224, 2004.
21. Zhang B, Lo C, Shen L, Sood R, Jones C, Cusmano-Ozog K, Park-Snyder S, Wong W, Jeng M, Cowan T, *et al*: The role of vanin-1 and oxidative stress-related pathways in distinguishing acute and chronic pediatric ITP. Blood 117: 4569-4579, 2011.
22. Berruyer C, Pouyet L, Millet V, Martin FM, LeGoffic A, Canonici A, Garcia S, Bagnis C, Naquet P and Galland F: Vanin-1 licenses inflammatory mediator production by gut epithelial cells and controls colitis by antagonizing peroxisome proliferator-activated receptor gamma activity. J Exp Med 203: 2817-2827, 2006.
23. Ryu S, Ornoy A, Samuni A, Zangen S and Kohen R: Oxidative stress in Cohen diabetic rat model by high-sucrose, low-copper diet: Inducing pancreatic damage and diabetes. Metabolism 57: 1253-1261, 2008.
24. Robertson RP, Harmon J, Tran PO, Tanaka Y and Takahashi H: Glucose toxicity in beta-cells: Type 2 diabetes, good radicals gone bad, and the glutathione connection. Diabetes 52: 581-587, 2003.
25. Piro S, Anello M, Di Pietro C, Lizzio MN, Patanè G, Rabuazzo AM, Vigneri R, Purrello M and Purrello F: Chronic exposure to free fatty acids or high glucose induces apoptosis in rat pancreatic islets: Possible role of oxidative stress. Metabolism 51: 1340-1347, 2002.
26. Wang M, Veeraperumal S, Zhong S and Cheong KL: Fucoidan-derived functional oligosaccharides: Recent developments, preparation, and potential applications. Foods 12: 878, 2023.
27. Pezzilli R and Pagano N: Is diabetes mellitus a risk factor for pancreatic cancer? World J Gastroenterol 19: 4861-4866, 2013.
28. Wang F, Larsson J, Adrian TE, Gasslander T and Permert J: In vitro influences between pancreatic adenocarcinoma cells and pancreatic islets. J Surg Res 79: 13-19, 1998.
29. Basso D, Brigato L, Veronesi A, Panozzo MP, Amadori A and Plebani M: The pancreatic cancer cell line MIA PaCa2 produces one or more factors able to induce hyperglycemia in SCID mice. Anticancer Res 15: 2585-2588, 1995.
30. Bonnefont-Rousselot D, Bastard JP, Jaudon MC and Delattre J: Consequences of the diabetic status on the oxidant/antioxidant balance. Diabetes Metab 26: 163-176, 2000.
31. Kaneto H, Katakami N, Kawamori D, Miyatsuka T, Sakamoto K, Matsuoka TA, Matsuhisa M and Yamasaki Y: Involvement of oxidative stress in the pathogenesis of diabetes. Antioxid Redox Signal 9: 355-366, 2007.
32. Butler PC, Meier JJ, Butler AE and Bhushan A: The replication of beta cells in normal physiology, in disease and for therapy. Nat Clin Pract Endocrinol Metab 3: 758-768, 2007.
33. Bensellam M, Jonas JC and Laybutt DR: Mechanisms of β-cell dedifferentiation in diabetes: Recent findings and future research directions. J Endocrinol 236: R109-R143, 2018.
34. Chang C, Su H, Zhang D, Wang Y, Shen Q, Liu B, Huang R, Zhou T, Peng C, Wong CC, *et al*: AMPK-dependent phosphorylation of GAPDH triggers Sirt1 activation and is necessary for autophagy upon glucose starvation. Mol Cell 60: 930-940, 2015.
35. Nakae J, Cao Y, Daitoku H, Fukamizu A, Ogawa W, Yano Y and Hayashi Y: The LXXLL motif of murine forkhead transcription factor FoxO1 mediates Sirt1-dependent transcriptional activity. J Clin Invest 116: 2473-2483, 2006.
36. Buteau J and Accili D: Regulation of pancreatic beta-cell function by the forkhead protein FoxO1. Diabetes Obes Metab 9 Suppl 2: 140-146, 2007.
37. Kitamura YI, Kitamura T, Kruse JP, Raum JC, Stein R, Gu W and Accili D: FoxO1 protects against pancreatic beta cell failure through NeuroD and MafA induction. Cell Metab 2: 153-163, 2005.
38. Talchai C, Xuan S, Lin HV, Sussel L and Accili D: Pancreatic β cell dedifferentiation as a mechanism of diabetic β cell failure. Cell 150: 1223-1234, 2012.
39. Matsuzaki H, Daitoku H, Hatta M, Aoyama H, Yoshimochi K and Fukamizu A: Acetylation of Foxo1 alters its DNA-binding ability and sensitivity to phosphorylation. Proc Natl Acad Sci USA 102: 11278-11283, 2005.
40. Aggarwal G, Ramachandran V, Javeed N, Arumugam T, Dutta S, Klee GG, Klee EW, Smyrk TC, Bamlet W, Han JJ, *et al*: Adrenomedullin is up-regulated in patients with pancreatic cancer and causes insulin resistance in β cells and mice. Gastroenterology 143: 1510-1517.e1, 2012.
41. Valerio A, Basso D, Brigato L, Ceolotto G, Baldo G, Tiengo A and Plebani M: Glucose metabolic alterations in isolated and perfused rat hepatocytes induced by pancreatic cancer conditioned medium: A low molecular weight factor possibly involved. Biochem Biophys Res Commun 257: 622-628, 1999.
42. Chai CY, Zhang Y, Song J, Lin SC, Sun S and Chang IW: VNN1 overexpression is associated with poor response to preoperative chemoradiotherapy and adverse prognosis in patients with rectal cancers. Am J Transl Res 8: 4455-4463, 2016.
43. Zhang L, Li L, Gao G, Wei G, Zheng Y, Wang C, Gao N, Zhao Y, Deng J, Chen H, *et al*: Elevation of GPRC5A expression in colorectal cancer promotes tumor progression through VNN-1 induced oxidative stress. Int J Cancer 140: 2734-2747, 2017.
44. Latre de Late P, El Wakil A, Jarjat M, de Krijger RR, Heckert LL, Naquet P and Lalli E: Vanin-1 inactivation antagonizes the development of adrenocortical neoplasia in Sf-1 transgenic mice. Endocrinology 155: 2349-2354, 2014.
45. Wang C, Huang B, Sun L, Wang X, Zhou B, Tang H and Geng W: MK8722, an AMPK activator, inhibiting carcinoma proliferation, invasion and migration in human pancreatic cancer cells. Biomed Pharmacother 144: 112325, 2021.
46. Park TH and Kim HS: Eupatilin suppresses pancreatic cancer cells via glucose uptake inhibition, AMPK activation, and cell cycle arrest. Anticancer Res 42: 483-491, 2022.

This work is licensed under a Creative Commons Attribution-NonCommercial-NoDerivatives 4.0 International (CC BY-NC-ND 4.0) License.